AD_____

Award Number: W81XWH-04-1-0222

TITLE: Analysis of Morphogenic Effect of hDAB2IP on Prostate Cancer and its Disease Correlation

PRINCIPAL INVESTIGATOR: Jer-Tsong Hsieh, Ph.D.

CONTRACTING ORGANIZATION: University of Texas, Southwestern Medical Center
Dallas, TX 75390-9110

REPORT DATE: February 2007

TYPE OF REPORT: Annual

PREPARED FOR: U.S. Army Medical Research and Materiel Command
Fort Detrick, Maryland 21702-5012

# REPORT DOCUMENTATION PAGE

*Form Approved*
*OMB No. 0704-0188*



| 1. REPORT DATE *(DD-MM-YYYY)* | 2. REPORT TYPE | 3. DATES COVERED *(From - To)* |
|---|---|---|
| 01-02-2007 | Annual | 1 Feb 2006 - 31 Jan 2007 |

**4. TITLE AND SUBTITLE**
Analysis of Morphogenic Effect of hDAB2IP on Prostate Cancer and its Disease Correlation

**5a. CONTRACT NUMBER**

**5b. GRANT NUMBER**
W81XWH-04-1-0222

**5c. PROGRAM ELEMENT NUMBER**

**6. AUTHOR(S)**
Jer-Tsong Hsieh, Ph.D.

E-Mail: JT.Hsieh@UTSouthwestern.edu

**5d. PROJECT NUMBER**

**5e. TASK NUMBER**

**5f. WORK UNIT NUMBER**

**7. PERFORMING ORGANIZATION NAME(S) AND ADDRESS(ES)**
University of Texas, Southwestern Medical Center
Dallas, TX 75390-9110

**8. PERFORMING ORGANIZATION REPORT NUMBER**

**9. SPONSORING / MONITORING AGENCY NAME(S) AND ADDRESS(ES)**
U.S. Army Medical Research and Materiel Command
Fort Detrick, Maryland 21702-5012

**10. SPONSOR/MONITOR'S ACRONYM(S)**

**11. SPONSOR/MONITOR'S REPORT NUMBER(S)**

**12. DISTRIBUTION / AVAILABILITY STATEMENT**
Approved for Public Release; Distribution Unlimited

**13. SUPPLEMENTARY NOTES**

**14. ABSTRACT:**
Imbalance of apoptotic and/or survival signaling cascade is a hallmark of malignant cell. In prostate cancer (PCa), constitutive activation of phosphatidylinositol 3-kinase (PI3K)-Akt/PKB and inactivation of apoptosis-stimulated kinase (ASK1)-JNK pathway signaling are often detected in metastatic cell. Understanding the underlying mechanism leading to such alternations will provide a better treatment strategy to control the terminal stage of this disease. In this project, we have proposed that DAB2IP protein, a novel RASGAP, is a part of homeostatic machinery and plays an important in modulating signal pathways elicited by exogenous survival/death stimuli. Our data clearly demonstrated that DAB2IP is a novel scaffold protein that complexes with key proteins involved in cell growth or death. The outcome of this study has led us to unveil a new mechanism of DAB2IP, which provides a better understanding how PCa cells switch from survival to death under the stimuli of exogenous signals.

**15. SUBJECT TERMS**
Cell differentiation, GTPase activating protein, tumor suppressor, Epigenetic regulation, signal transduction, prostate cancer

| 16. SECURITY CLASSIFICATION OF: | | | 17. LIMITATION OF ABSTRACT | 18. NUMBER OF PAGES | 19a. NAME OF RESPONSIBLE PERSON |
|---|---|---|---|---|---|
| a. REPORT | b. ABSTRACT | c. THIS PAGE | | | USAMRMC |
| U | U | U | UU | 22 | 19b. TELEPHONE NUMBER *(include area code)* |

**Standard Form 298 (Rev. 8-98)**
**Prescribed by ANSI Std. Z39.18**

**Table of Contents**

## INTRODUCTION

Expression of Ras protein has also been assessed in primary and metastatic prostate cancer (PCa) tumors. Most tumors expressed higher Ras protein than normal prostate tissues (1). Also, an increased c-H-Ras mRNA expression in PCa is associated with the progression of PCa to androgen independence (2). Surprisingly perhaps, PCa specimens from American men have an extremely low rate of mutation in the Ras gene (3). This implies that other effectors may be involved in increasing RAS protein levels in PCa. DAB2IP appears to be a good candidate because it contains an amino acid sequence that is homologous to the GTPase activating protein (GAP) domain of other RasGAPs and it is functional active based on biochemical and molecular biologic studies (4). In addition to the GAP domain, DAB2IP contains several other functional motifs such as a pleckstrin homology domain (aa 20-70) with a high affinity to certain phosphoinositides, a C2 domain (aa 90-120) involved in binding phospholipids in a calcium-dependent or -independent manner, a proline-rich (PR) domain (aa 796-805) involved in interacting with proteins that contain a SH3 domain, and a leucine zipper (aa 842-861), which mediates dimerization. For example, the C2 domain of DAB2IP can bind and then activate apoptosis-stimulated kinase (ASK1) involved in the TNF-α-mediated apoptosis (5).

In addition to the interaction of C2 domain with ASK1, DAB2IP mutants defective in GAP activity failed to increase ASK1 activity, suggesting that the GAP activity of DAB2IP is required for TNF-α-elicited ASK1 activity (5). Also, the GAP activity of DAB2IP is known to be a negative regulator for Ras-Raf-ERK activation critical for cell growth. Thus, DAB2IP appears as a unique factor in modulating both cell growth and death by inhibiting Ras-Raf-ERK proliferative pathway (6) and activating ASK1-JNK/p38 apoptotic signaling. Very likely, other functional domains in DAB2IP have different roles in maintaining homeostasis of prostate epithelium.

## RECENT PROGRESS

Overall, Task 1 and 2 are completed and Task 3 is completed 60%. In summary, we made several key progresses in this project: (1) Loss of DAB2IP expression is associated with the recurrent of androgen-independent (AI) PCa; (2) Loss of DAB2IP expression is mainly due to epigenetic regulation; (3) DAB2IP is a key homeostatic factor in balancing cell growth and aoptosis. Thus, I have summarized these new results as follows:

### Task 3. To delineate signal cascade mediated by hDAB2IP protein complex in prostatic epithelium.

**The role of DAB2IP in modulating cell survival and death**

Cell homeostasis is a balance between cell proliferation, apoptosis and differentiation in basal and luminal epithelia. It is believed that loss of homeostatic control in these cells renders the onset of neoplasm in prostatic epithelium. Until now, a little is known about homeostatic machinery in normal prostatic epithelium. Recently, we identified DAB2IP as a new member of GTPase activating protein (GAP) family as a potent growth inhibitor in metastatic PCa cell lines (7) by inducing $G_0$ cell cycle arrest and promoting apoptosis under stress factor (Fig. 1). It is known that the C2 domain can interact with ASK1 to facilitate TNF-α-mediated apoptosis by activating ASK1. Our preliminary data further indicated that the PR domain in DAB2IP is

critical for binding PI3K regulatory subunit (p85) and then suppresses the activation of Akt (Fig. 2); the first six amino acids of PR domain appear to be key binding site (Fig. 3). It appears that DAB2IP-mediated Akt inactivation can concomitantly enhance ASK1 activation leading to cell apoptosis. In contrast, DAB2IP siRNA can restore Akt activity, suppress ASK1 activation and reduce apoptosis (Fig. 4), indicating that DAB2IP is critical factor for interaction between Akt and ASK1. Taken together, we believe that DAB2IP is a novel scaffold protein for both survival and death signal molecules, by which DAB2IP complex is a key machinery to maintain homeostasis in normal cell.

**Figure 1 The role of DAB2IP in PI3K inhibitor (LY294002)-induced cell apoptosis.** DAB2IP-transfected PCa lines (C4-2) were determined for DAB2IP expression (a), then the total cell number (b), the percentage of apoptotic cell (c) and apoptotic hallmark-PARP cleavage (d) were determined after 24 hrs of treatment.

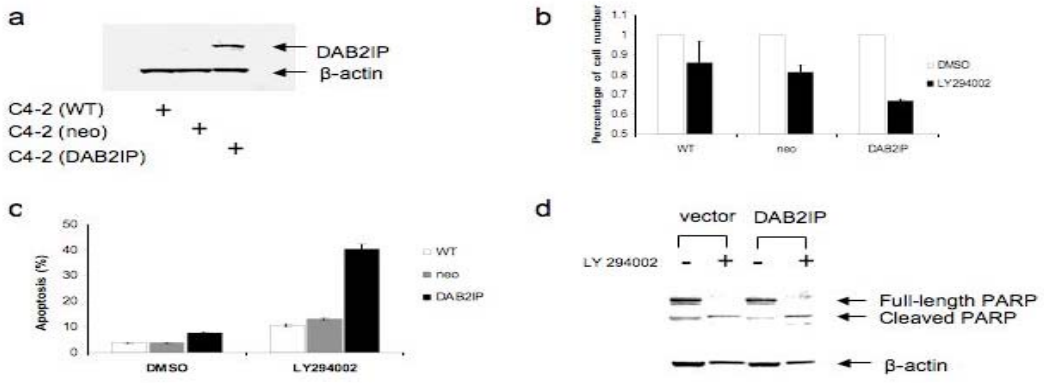


**Figure 2 The level of phosphorylated Akt and total Akt in DAB2IP-transfected C4-2.** Cells were treated LY294002 (10 μM) (a) or TNF-α (100 ng/ml) (b) for 30 min and total cell lysate was subjected to western blot analysis.

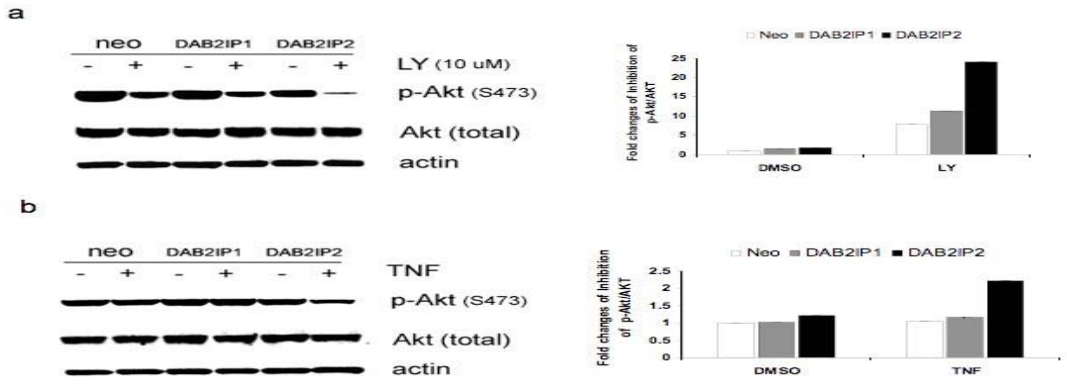


**Figure 3 Determination of interactive domain in DAB2IP with the regulatory domain PI3K (p85)**. Using pull down (a) or immunoprecipitation (b), the first six amino acids in PR domain of DAB2IP is a critical binding domain with p85. The mutant can diminish the activity of DAB2IP in LY294002- or TNF-α-elicited cell apoptosis.

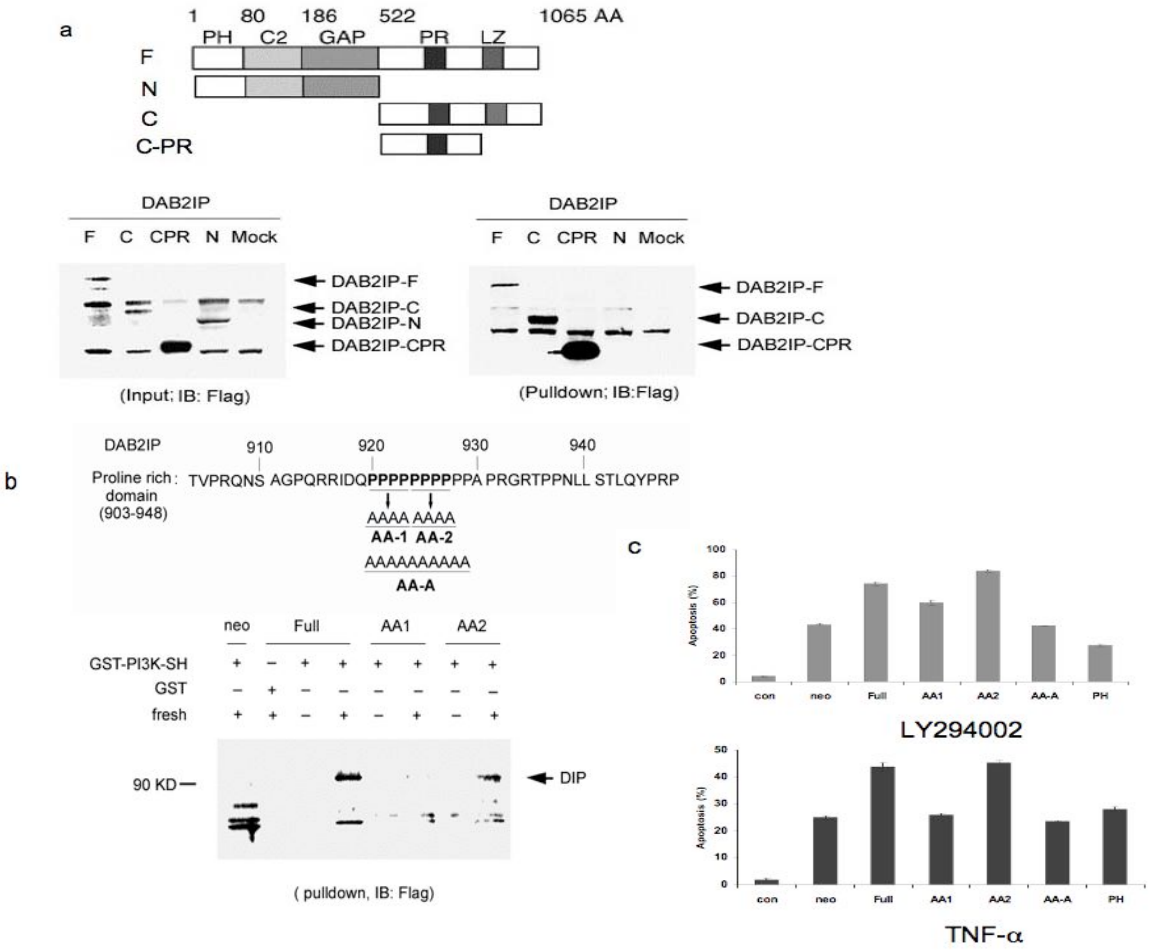


**Figure 4 Reduction of LY294002- or TNF-α̃-mediated cell apoptosis by DAB2IP siRNA.** Endogenous DAB2IP levels in PZ-HPV7 was decreased by DAB2IPsiRNA (a), which resulted in elevated activated Akt (b), decreased activated ASK1 (c) and decreased cell apoptosis (d̃) after treating with LY294002- or TNF-α.

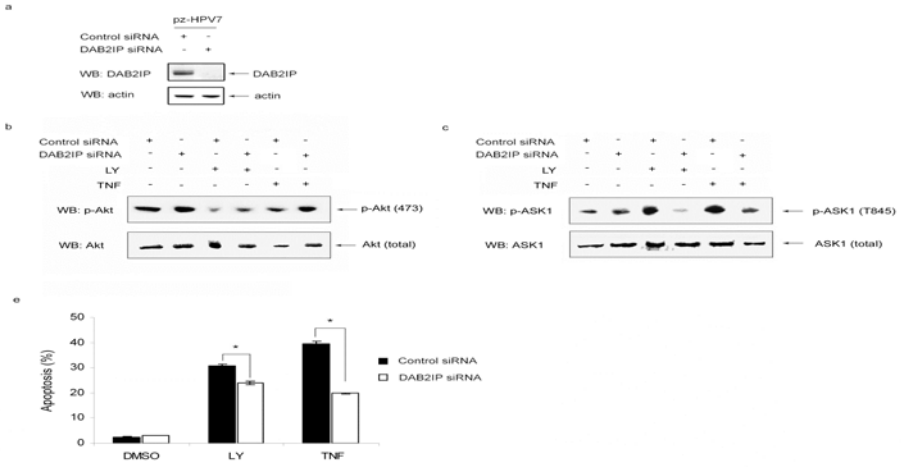

## KEY RESEARCH ACCOMPLISHMENT

- Clone mouse DAB2IP gene, map the promoter region and characterize epigenetic regulation (**This work has been published on the cover page of DNA and Cell Biology journal**).
- Generate a series of DAB2IP mutant constructs.
- Generate a DAB2IP knock out ES cell.
- Map new functional domain in DAB2IP for controlling cell survival.
- Determine the role of DAB2IP in cell survival/ apoptosis of PCa cells by various exogenous stimuli.

## REPORTABLE OUTCOMES


1. Chen, H, Karam. J.A., Schultz, R., Zhang, Z., Ducan, C., and Hsieh, J.T. (2006) Cloning of *mDAB2IP* gene, a novel member of the RasGTPase-activating protein family and characterization of its regulatory region. DNA and Cell Biol., 25: 232-245.
2. Hsieh, J.T., Karam, J.A., and Min, W. (2007) The Link of Genetic and Biologic Evidence from DAB2IP gene with Aggressive Prostate Cancer. JNCI, (submiited).


## CONCLUSIONS

Prostate homeostasis relies on a balance between cell proliferation, apoptosis and differentiation. We initially identified DAB2IP, a novel Ras-GTPase activating protein (Ras-GAP), as a DOC-2/DAB2-interacting protein from a yeast two-hybrid system. A blast search indicated that DAB2IP consists of several conserved structural domains –the pleckstrin homology (PH), the protein kinase C conserved region 2 (C2) and RasGAP at the N-terminal half, and at the C-terminal half a proline-rich sequence (PR) and a leucine-zipper motif (LZ). We have extensively characterized the structural and functional relationship of AIP1 involved in the TNF signaling pathways. Interestingly, DAB2IP mutants defective in GAP activity failed to increase ASK1 activity, suggesting that the GAP activity of AIP1 is required for AIP1-enhanced ASK1 activity. The GAP activity of Ras-GAP is known to be critical for regulation of Ras-Raf-ERK activation. The requirement for AIP1 GAP activity in ASK1-JNK activation is supported by observation that ERK exerts an inhibitory effect on ASK1-JNK signaling. Crosstalk among MAPKs, i.e. one MAPK (e.g. ERK) may inhibit or oppose the activation of another MAPK (e.g, JNK), has been well documented. Many stimuli reciprocally regulate ERK and JNK activation Conversely, ERK inhibition by DAB2IP (via GAP activity) may require for DAB2IP-enhanced ASK1-JNK activation. Now, our data have further established a linkage of PI3K, Ras-GAP to stress-activated ASK1-JNK signaling pathway. Further study of the role of DAB2IP in signal transduction will provide more understanding of recurrent AIPCa.

**REFERENCES**


1. Bushman EC, Nayak RN, Bushman W. Immunohistochemical staining of ras p21: staining in benign and malignant prostate tissue. J Urol. 1995; 153:233-7.
2. Bakin RE, Gioeli D, Bissonette EA, Weber MJ. Attenuation of Ras signaling restores androgen sensitivity to hormone-refractory C4-2 prostate cancer cells. Cancer Res 2003; 63:1975-80.
3. Konishi N, Hiasa Y, Tsuzuki T, Tao M, Enomoto T, Miller GJ. Comparison of ras activation in prostate carcinoma in Japanese and American men. Prostate. 1997; 30:53-7.
4. Wang Z, Tseng CP, Pong RC, Chen H, McConnell JD, Navone N, et al. A Novel RasGTPase activating protein that interacts with DOC-2/DAB2: A downstream effector leading to the suppression of prostate cancer. J Biol Chem 2002; 277: 12622-31.
5. Zhang R, He X, Liu W, Lu M, Hsieh JT, Min W. AIP1 mediated TNF-induced ASK1 activation by facilitating dissociation of ASK1 from inhibitor 14-3-3. J. Clin. Invest 2003; 11:1933-43.
6. Zhou J, Scholes J, Hsieh JT. Signal transduction targets in androgen independent prostate cancer. Cancer and Metastasis Review, 2001; 20:351-362.
7. Wang Z, Tseng CP, Pong RC, Chen H, McConnell JD, Navone N, et al. A Novel RasGTPase activating protein that interacts with DOC-2/DAB2: A downstream effector leading to the suppression of prostate cancer. J Biol Chem 2002; 277: 12622-31.

DNA AND CELL BIOLOGY
Volume 25, Number 4, 2006

Pp. 232–245

# Cloning of Mouse *Dab2ip* Gene, a Novel Member of the RasGTPase-Activating Protein Family and Characterization of Its Regulatory Region in Prostate

HONG CHEN,[1] JOSE A. KARAM,[1] ROGER SCHULTZ,[2] ZHENGWANG ZHANG,[1] CHRISTINE DUNCAN,[2] and JER-TSONG HSIEH[1]

## ABSTRACT

**Disabled homolog 2 (*Drosophila*) interacting protein (DAB2IP/Dab2IP) is a member of the GTPase-activating protein for downregulating the Ras-mediated signal pathway and TNF-mediated apoptosis. The downregulation of human *DAB2IP* mRNA levels was detected in prostate cancer cells due to the epigenetic regulation. Here, we isolated a mouse *Dab2ip* gene with a highly homologous sequence to that of the human and rat gene and mapped it at chromosome 2B. The *mDab2ip* gene contains 14 exons and 13 introns and spans approximately 65 kb. Exon1 contains at least three splicing variants (Ia, Ib, and Ic). The deduced amino acid sequence of mouse Dab2IP encompasses 1065 residues containing several unique protein interaction motifs as well as a Ras-like GAP-related domain, which shares a high homology with both humans and rats. Data from real-time RT-PCR analysis revealed a diverse expression pattern of the *mDab2ip* gene in various organs, implying differential regulation of this gene from various tissues. We have mapped a 1.3-kb segment containing a 5′-upstream region from exon Ia as a promoter region (−147/+545) in prostatic epithelial cell lines (TRAMP-C); this region is highly GC-rich, and *mDab2ip* appears to be a TATA-less promoter. It appears that epigenetic regulation, particularly histone acetylation of the *Dab2ip* gene promoter, plays an important role in modulating its gene expression in the mouse prostate cancer cell.**

## INTRODUCTION

DISABLED HOMOLOG 2 (*Drosophila*) interacting protein (DAB2IP/Dab2IP) is a novel member of the Ras GTPase-activity family protein (Chen *et al*., 2002; Wang *et al*., 2002) DAB2IP is able to interact with DOC-2/DAB2 (Fulop *et al*., 1998; Tseng *et al*., 1999; Zhou and Hsieh, 2001; Zhou *et al*., 2003), and this protein complex modulates the Ras-mediated signal pathway, then causes the growth inhibition in prostate cancer cells (Wang *et al*., 2002). Also, DAB2IP (also named AIP1: ASK interacting protein 1) is involved in TNF-$\alpha$-mediated cell apoptosis by facilitating dissociation of ASK1 from its inhibitor 14-3-3 (Zhang *et al*., 2003, 2004)

The higher *hDAB2IP* mRNA levels are detected in normal human prostatic epithelium than in prostate cancer cells, which is due to the epigenetic regulation (Wolffe and Matzke, 1999; Jones and Takai, 2001) such as DNA methylation and histone acetylation of the human *DAB2IP* (*hDAB2IP*) gene promoter (Chen *et al*., 2002, 2003). In breast cancer, DNA hypermethylation of *hDAB2IP* is also found in both breast cancer cell lines and specimens with lymph node metastasis, and *hDAB2IP* gene expression can be restored in methylated cell lines treated with 5-aza-2′-deoxycytidine (Dote *et al*., 2004). Also, *hDAB2IP* (alias for AFQ34) is identified as a novel MLL fusion partner from an acute myeloid leukemia (AML) patient with a t(9;11)(q34;q23); the intron 9 of the MLL gene is translocated into the exon 2 of *DAB2IP*, and causes the disruption of the pleckstrin homology (PH) domain in the DAB2IP protein, implying that this fusion protein may alter RAS activity as a part of leukemia transformation process (von Bergh *et al*., 2004). Thus, DAB2IP should be involved in carcinogenesis of various tissues.

To further unveil the physiological functions of mouse *Dab2ip*, we decided to clone and map its chromosomal location. With analyzing the structure of the mouse *Dab2ip* (*mDab2ip*) gene, we have assembled the entire gene sequence and its full-length mRNA with an open reading frame. We also

Departments of [1]Urology and [2]Pathology, University of Texas Southwestern Medical Center, Dallas, Texas.

profiled the *mDab2ip* expression pattern from a variety of organs and cell lines. By determining the promoter sequence from the 5'- flanking region of the *mDab2ip* gene in mouse prostatic epithelial cell lines provided clues for the transcriptional regulation of the *mDab2ip* gene.

## MATERIALS AND METHODS

### *Tissue culture, treatment, and RNA isolation*

Three mouse transgenic prostate adenocarcinoma cell lines (TRAMP-C1, TRAMP-C2, and TRAMP-C3) (Greenberg *et al*., 1995; Foster *et al*., 1997; Gingrich *et al*., 1997) were maintained in DMEM supplemented with 5% FBS (HyClone, Logan, UT) plus 5% Nu-serum™ IV (BD Bioscience, Bedford, MA) and 50 ng/ml insulin (Sigma St. Louis, MO). The NIH-3T3 cell line was maintained in DMEM with 10% fetal bovine serum (FBS), and the PC3 cell line was maintained in T medium supplemented with 5% FBS. Total RNA from variant organs and cell lines were isolated using the RNAzol B (Tel-Test Inc., Friendswood, TX) according to the manufacturer's instructions.

For tissue RNA isolation, various organs (approximate 50 mg) were harvested from nude mice after euthanasia and were snap-frozen in liquid nitrogen until analysis was performed. Tissues were submerged with RNAzol B, quickly homogenized, then subjected to the same isolation procedure.

To study the effect of hisone acteylation, different concentrations (20, 40, and 100 nM) of Trichostatin (TSA), a histone deacetylase (i.e., HDAC) inhibitor, was changed every 24 h for 48 h. For studying the effect of DNA methylation, different concentrations (1, 2, and 5 $\mu$M) of 5-aza-2′-deoxycytidine (5′-Aza), a DNA methyltransferase (DNMT) inhibitor, was changed every 48 h for 96 h. For the combination, 5′-Aza was first added and changed every 48 h; then TSA was added 72 h after treatment. Cells were collected at 96 h after treatment.

### *Cloning mouse* Dab2ip *gene and sequence analysis*

To obtain the entire coding region of mouse *Dab2ip* cDNA, we performed RT-PCR from total cellular RNA from the mouse brain. Based on the high homology sequences between human and rat *DAB2IP* cDNA (Chen *et al*., 2002; Wang *et al*., 2002), two sets of primer were synthesized (Table 1). PCR products were cloned into pCR2.1-TOPO vector (Invitroge, Carlsbad, CA) and sequenced, then used as probes for screening the *mDab2ip* gene.

A mouse bacterial artificial chromosomal (BAC, RPCI.22) library (ResGen Invitrogen Corp., Huntsville, AL) was screened. The positive clones were subjected to Southern blot analysis and DNA sequencing for confirmation.

TABLE 1. PCR PRIMERS USED ON 5′ RACE, REAL-TIME RT-PCR, PROBE AND PROMOTER CONSTRUCTS

| *Application* | *Primer name* | *Primer 5′–3′ sequence* |
|---|---|---|
| 5′ RACE | Sp1 (outer) | ATACAGCACATCGTCCAGG |
| | Sp2 (inner) | GTTCTCCATCCACTTATCGCGC |
| Real-time RT-PCR | F-mDab2ip | CGATAAGTGGATGGAGAACCTGAG |
| | R-mDab2ip | AGATGCTGACGGTCTGGTAGCGTGC |
| | F-Actin | TGTGTGGATTGGTGGCTCTATC |
| | R-Actin | CTGCTTGCTGATCCACATCTG |
| Probe 1 (800 bp) | F1-*DAB2IP* | TCGTGGAAGGACTCATGACC |
| | R1-*DAB2IP* | TCCACCACCCTGTTGCTGTA |
| Probe 2 (300 bp) | F2-*DAB2IP* | TGGACGATGTGCTCTATGCC |
| | R2-*DAB2IP* | GGATGGTGATGGTTTGGTAG |
| Promoters | F1 | GCTCCTCACCTGCCTCTTCATTAG |
| | F6 | CCTGCTCTCCCAGCCTTAGTTTC |
| | F8 | CACCAAGAGCCAGCCCAAAC |
| | F10 | ACCCTTCGTTGCTTTCACCG |
| | F12 | GAGTCCCTCGCTGTCCGATAC |
| | R2 | TGCTCCTCCCCTCCAGATGTTC |
| Mutagenesis | F-ΔSp1 | GGCGGGGGCGACGGGCCGCGAGGG |
| | R-ΔSp1 | CCCTCGCGGCCCGTCGCCCCCGCC |
| | F-ΔAP2 | CCTTCCCCCTCTTGCAGGGCTTCCTCAG |
| | R-ΔAP2 | CTGAGGAAGCCCTGCAAGAGGGGGAAG |
| Bisulfite-treated DNA | Fm | ATTAAGAGTTAGTTTAAATTGGAT |
| | Rm | ACCTCCAACACCCTCCTAAATAC |
| Immunoprecipitated DNA (ChIP) | F (outer) | CCTGCTCTCCCAGCCTTAGTTTC |
| | R (outer) | TGTGGTTGCGGTCCAGTTTG |
| | F (inner) | ATGGCAACGGCGGCTTAGG |
| | R (inner) | TTTGGGCTGGCTCTTGGTG |

### *Identification of transcriptional starting site (TSS) by 5′ RACE*

To determine the transcriptional starting site of the *mDab2ip* gene, the total cellular RNA (10 $\mu$g) from two mouse organs (the brain and kidney) and two TRAMP-C lines (TRAMP-C1 and TRAMP-C2) was subjected to 5′ RACE using the FirstChoice™ RLM-RACE Kit (Ambion Inc., Austin, TX) according to the manufacturer's manual. A random-primed reverse-transcription reaction and nested PCR (Fig. 2B and Table 1) were performed to amplify the 5′end of the *mDab2ip* mRNA transcript. We analyzed the PCR product in a 2% NuSieve® 3:1 agarose gel (Cambrex BioScience, Rockland, MA) and then cloned it into pCR2.1-TOPO for sequence identification.

### *Determination of mDAB2IP mRNA levels by real-time quantitative RT-PCR (qRT-PCR) assay*

Two micrograms of total cellular RNA were reversely transcribed into cDNA and amplified using either the *mDab2ip* primer set (2 ng/$\mu$l) or *Actin* primer set (6 ng/$\mu$l) (Table 1) in a 40-$\mu$l reaction mixture containing 20-$\mu$l IQ™ SYBR® Green Supermix (Bio-Rad, Hercules, CA). The PCR was performed using an iCycler machine (Bio-Rad) and the reaction condition was as follow: 95°C (3 min) and 40 cycles amplification cycle (95°C [30 sec], 55°C [30 sec], and 72°C [1 min]). To assure the quality of each reaction, melting curves analysis was performed using 95°C (1 min), 55°C (1 min), and 80 cycles of 0.5°C increment beginning at 55°C. Each sample was performed in duplicate. The level of *mDab2ip* mRNA from each organ was calculated as follows: $\Delta Ct$ (threshold cycle) of each sample = mean of $C_{t(Dab2ip)}$ − mean of $C_{t(Actin)}$. The relative expression of *mDab2ip* in each organ was calculated as $1/2^{\Delta Ct(\text{sample tissue})} - \Delta Ct(\text{spleen})$, since the spleen had the lowest *Dab2ip* mRNA level. Meanwhile, the levels of the *mDab2ip* mRNA from each cell line were calculated as $1/2^{\Delta Ct(\text{sample cell})} - \Delta Ct(\text{TRAMP-C3})$, since TRAMP-C3 had the lowest expression of *mDab2ip*.

### *Fluorescence* in situ *hybridization (FISH) analysis*

To determine the chromosomal localization of the *mDab2ip* gene, cells were sterilely isolated from the spleens of 6-week-

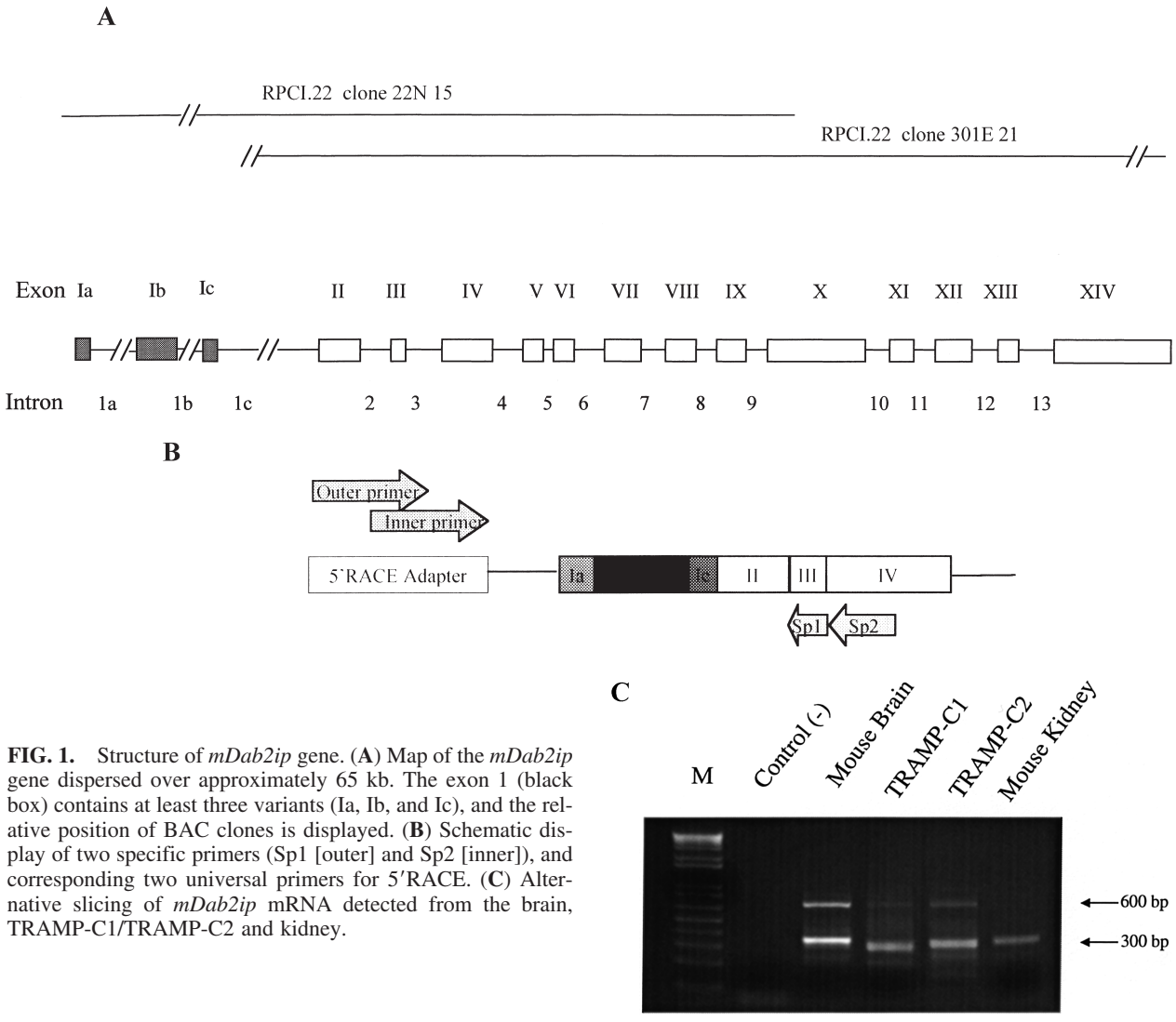


**FIG. 1.** Structure of *mDab2ip* gene. (**A**) Map of the *mDab2ip* gene dispersed over approximately 65 kb. The exon 1 (black box) contains at least three variants (Ia, Ib, and Ic), and the relative position of BAC clones is displayed. (**B**) Schematic display of two specific primers (Sp1 [outer] and Sp2 [inner]), and corresponding two universal primers for 5′RACE. (**C**) Alternative slicing of *mDab2ip* mRNA detected from the brain, TRAMP-C1/TRAMP-C2 and kidney.

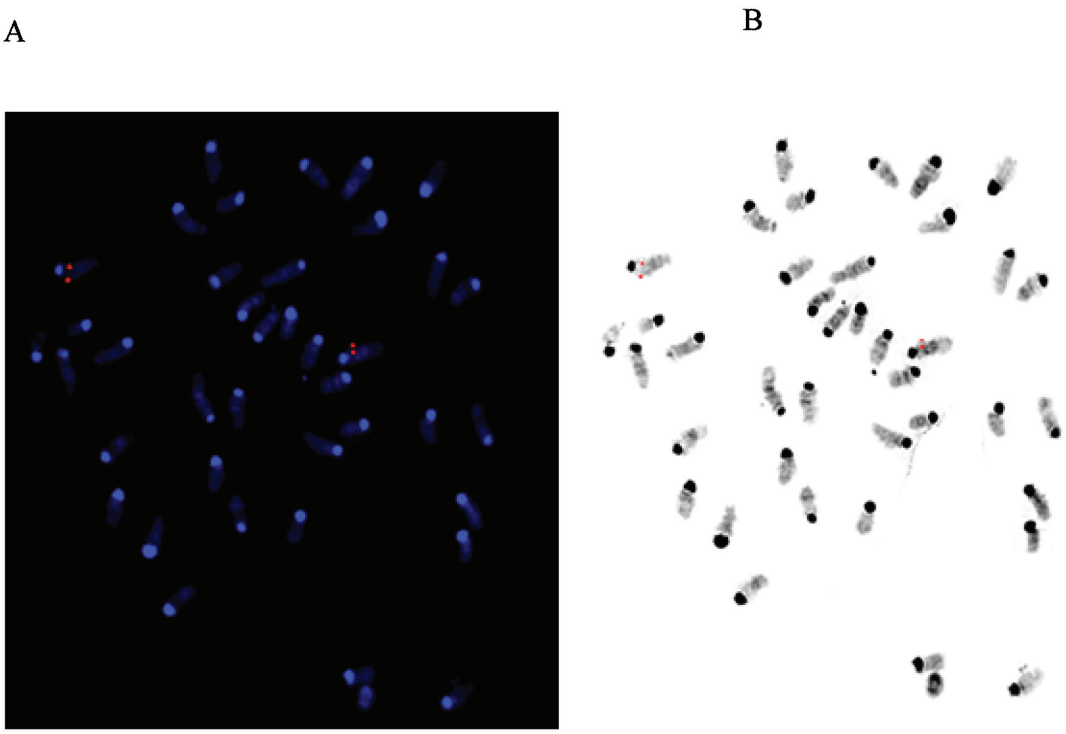


**FIG. 2.** Chromosomal localization of the *mDab2ip* gene by FISH analysis. (**A**) A DAPI stained chromosomes (blue) with hybridized probe (red), and (**B**) a reversed image of the chromosomal staining.

old mice and set up in RPMI 1640 with glutamine, 20% FBS, and 50 $\mu$g lipopolysaccharide at 37°C for 42 h. At 42 h 0.75 $\mu$l of 10 $\mu$g/ml colcemid was added and incubated for 10 min. Cells were pelletted, resuspended in 1 ml of hypotonic KCl (prewarmed to 37°C), and incubated at room temperature for 15 min. The cells were then fixed in methanol:acetic acid (3:1) and spread on slides using heat treatment. DNA probes from BAC clones 22N15 and 301E21 were fluorescently labeled by nick translation using standard conditions. The probe was hybridized to mouse metaphase slides overnight in a HYBrite (Vysis, Inc., Downers Grove, IL) hybridization chamber and washed. The hybridization signal was viewed and analyzed on an Olympus AX70 fluorescence microscope and images captured using MacProbe software (version 4.4, Applied Imaging, San Jose, CA).

### *Construction of luciferase reporter plasmid containing the 5′-upstream regulatory sequence of the* mDab2ip *gene*

To analyze the 5′-upstream regulatory sequence of the *mDab2ip* gene, a 1.3-kb fragment from −730 to +545 (transcription initial site as +1 predicted by 5′RACE data) containing the upstream region, exon Ia and partial intron 1a was amplified by PCR from clone 22N15. To further define the promoter region in the *mDab2ip* gene, a series of deletion mutants were generated by PCR (Table 1). The PCR products were subcloned into the pCR(-Blunt II TOPO vector (Invitrogen, Carlsbad, CA). After sequencing confirmation, they were further cloned a into pGL3 basic vector (Promega, Madison, WI) using *Kpn*I/*Xho*I sites to generate pGL3–F1/R2 (from −730 to +545), pGL3–F6/R2 (from −421 to +545), pGL3–F8/R2 (from +6 to +545), pGL3–F10/R2 (from +249 to +545), pGL3–F12/R2 (from +445 to +545), The pGL3–F7/R2 contains a *Nco*I fragment (from −147 to +545) of *mDab2ip*. The pGL3–F6/*Nco*I contains a 0.3-kb insert from −421 to −157 and pGL3-F6/*San*DI contains a 0.4-kb insert from-421 to −97.

For mutagenesis studies, we used pGL3–F7/R2 as a template to generate deletion mutants: pGL3–ΔSp1 (deletion of potential Sp1 site from −124 to −114) and pGL3–ΔAP2 (deletion of potential AP2 site from −47 to −26) using a Quikchange® II XL Site-Directed Mutagenesis Kit (Stratagene, La Jolla, CA) with the primer set (Table 1).

### *Measurement of* mDab2ip *putative promoter activity using reporter gene assay*

Both TRAMP-C1 and TRAMP-C3 were plated at a density of $0.6 \times 10^5$ cells per well in a six-well plate. After 16 h, cells were transfected with both 0.8 $\mu$g of reporter vectors and the 0.2 $\mu$g $\beta$-galactosidase ($\beta$-gal) vector (pCH110) using Lipofectamine Plus transfection reagent (Invitrogen). Twenty-four hours after incubation, the transfected cells were treated with TSA for 24 h, 5′-Aza for 48 h, or a combination of both drugs by incubating 5′-Aza for 24 h then adding TSA for an additional 24 h. Cells were washed twice with cold phosphate-buffered saline (PBS) and harvested them in lysis buffer (Promega); then cell lysate was subjected to luciferase and $\beta$-gal assays as described previously (Chen *et al*., 2003). The relative luciferase activity (RLA) from each sample was determined by normalizing the luciferase activity with its $\beta$-gal activity. All experiments were repeated at least three times in triplicate.

### *Chromatin immunoprecipitation (ChIP) assay*

Chromatin Immunoprecipitation (ChIP) assay was performed as described previously (Chen *et al*., 2003) with a specific PCR primer set (Table 1). Precleared chromatin from $2 \times 10^6$ cells was used for each ChIP sample. The 5-$\mu$g anti-Acetyl Histone H3 (Upstate, Lake Placid, NY) antibodies were used in the per ChIP assays. The immunoprecipitated DNA was amplified by genomic-PCR, and the PCR products were subjected to gel electrophoresis.

### *Bisulfite genomic sequencing*

High molecular weight genomic DNA was obtained from NIH-3T3, TRAMP-C1, TRAMP-C2, and TRAMP-C3 cell lines and subjected to bisulfite modification as previously described (Chen *et al*., 2003). Bisulfite-modified DNA was amplified by PCR with specific primer set (Table 1). The PCR products were further subcloned into a TA cloning vector pCR2.1-TOPO, and at least five individual clones were sequenced using a reverse M13 primer.

## RESULTS

### *Characterization of the* mDab2ip *gene*

A mouse bacterial artificial chromosomal (BAC) library was screened with two partial *mDab2ip* cDNA probes. Three positive clones were identified (22N15, 301E21, and 538A16). Two of them (22N15 and 301E21) were chosen for further study because both contained the *mDab2ip* gene confirmed by PCR and Southern blot analysis using a 800-bp partial *mDab2ip* cDNA probe (data not shown). We performed sequencing analysis using Sp6 and T7 primers to analyze both clones. With the BLAST program (National Center for Biotechnology Information [NCBI], http://www.ncbi.nlm.nih.gov), we matched these two clones with the *Mus musculus* chromosome 2 genomic contig sequence (accession no. NT_039206). The sequence data showed the 3'end sequencing (T7 primer) of clone 22N15 aligned with the middle portion of the *mDab2ip* gene and the 5′ end sequence (Sp6 primer) aligned with 5′ upstream of NT_039206. The sequence of clone 301E 21 spans the entire *mDab2ip* gene except the 5′ upstream regulation region (Fig. 1A). Furthermore, we performed flourescence *in situ* hybridization (FISH) analysis using 22N15 and 301E21 as probes; we were able to locate the *mDab2ip* gene at chromosome 2B (Fig. 2A and B).

We deduced the exon–intron junction of *mDab2ip* by aligning its cDNA sequence with NT_039206. Furthermore, we confirmed all predicted exon–intron boundaries by PCR and DNA sequencing, which junction coincides with the GT . . . AG rule. It appears that the *mDab2ip* gene contains 14 exons and 13 introns (Fig. 1A and Tables 2 and 3). Noticeably, exon 1 is a noncoding exon that was separated from exon 2 by a large intron (>10 kb). The translation initiation site (ATG) is mapped at the 11-bp downstream from the 5′-end of exon 2 and the protein termination site (TAA) is located at exon 14 followed with a large untranslated sequence.

To further determine the transcription starting site(s) of the *mDab2ip* gene, we designed two *mDab2ip*-specific primers (Sp1, Sp2) to combine with universal outer and inner adapter primers for nested PCR (Fig. 1B). As shown in Figure 1C, two PCR transcripts (300 and 600 bp) were detected from RNA isolated from the mouse brain and two mouse prostatic epithelial cell lines (TRAMP-C1 and -C2). In contrast, only one single transcript (300 bp) was detected from kidney RNA. DNA sequencing data revealed at least three variants form the exon 1. The *mDab2ip* mRNA from the mouse brain and TRAMP-C contains both exon Ia and exon Ib; the *mDab2ip* mRNA from the mouse kidney contains exon Ic.

### *A high homology of deduced protein sequence among mouse Dab2IP, and human, and rat DAB2IP*

In our recent study (Chen *et al*., 2002), we show that the deduced Dab2IP protein sequence is remarkably similar between

TABLE 2. DIFFERENT SPLICING VARIANTS OF MOUSE *DAB2IP*

| *Exon* | *mDab2ip mRNA a (6109bp)* | *mDab2ip mRNA b (6392bp)* | *mDab2ip mRNA c (6051bp)* | *Amino acid (1065aa)* |
|---|---|---|---|---|
| Ia | 1–134 | | | |
| Ib | | 1–417 | | |
| Ic | | | 1–76 | |
| II | 135–288 (154) | 418–571 (154) | 77–230 (154) | 1–48 (48) |
| | ***ATG (145–147)** | ***ATG (428–440)** | ***ATG (87–89)** | |
| III | 289–387 (99) | 572–670 (99) | 231–329 (99) | 49–81 (33) |
| IV | 388–942 (555) | 671–1225 (555) | 330–884 (555) | 82–266 (185) |
| V | 943–1087 (145) | 1226–1370 (145) | 885–1029 (145) | 267–314 (48) |
| VI | 1088–1232 (145) | 1371–1515 (145) | 1030–1174 (145) | 315–363 (49) |
| VII | 1233–1469 (237) | 1516–1752 (237) | 1175–1411 (237) | 364–442 (79) |
| VIII | 1470–1671 (202) | 1753–1954 (202) | 1412–1613 (202) | 443–509 (67) |
| IX | 1672–1850 (179) | 1955–2133 (179) | 1614–1792 (179) | 510–569 (60) |
| X | 1851–2739 (889) | 2134–3022 (889) | 1793–2681 (889) | 570–865 (296) |
| XI | 2740–2892 (153) | 3023–3175 (153) | 2682–2834 (153) | 866–915 (50) |
| XII | 2893–3086 (194) | 3176–3369 (194) | 2835–3028 (194) | 916–981 (66) |
| XIII | 3087–3174 (88) | 3370–3457 (88) | 3029–3116 (88) | 982–1010 (29) |
| XIV | 3175–6109 (2935) | 3458–6392 (2935) | 3117–6051 (2935) | 1011–1065 (55) |
| | ***TAA (3340–3342)** | ***TAA (3623–3625)** | ***TAA (3282–3284)** | |

TABLE 3. EXON–INTRON BOUNDARIES OF THE MOUSE DAB2IP

| *Exon* | *Size (bp)* | *3′ intron/5′ exon boundary* | *3′ exon/5′ intron boundary* | *Intron* | *Size (kb)* |
|---|---|---|---|---|---|
| Ia | 134 | | TGAGAG/gtaggccc | 1a | 29.3 |
| Ib | 417 | cctcctcag/GTCCCA | GCCAAG/gtctgtgac | 1b | 4.3 |
| Ic | 76 | cctcctcag/GTCCCA | CACTTG/gtgagtggc | 1c | 10.0 |
| II | 154 | cctcctcag/GTCCCA | TTCGAG/gtgggtgtc | 2 | 1.0 |
| III | 99 | gtttgacag/GTGACG | AACAAG/gtacctgta | 3 | 0.9 |
| IV | 555 | cttatgcag/GACAAC | GTGAAG/gtgagtgtg | 4 | 2.7 |
| V | 145 | cctccctag/GACTTT | CACTAG/gtagtgggg | 5 | 0.1 |
| VI | 145 | gcccacag/GTGAGT | CTACTG/gttagtgcca | 6 | 2.7 |
| VII | 237 | cctatgcag/TGCTTC | TGCCAA/gtgagtgtt | 7 | 1.6 |
| VIII | 202 | ttctgtccag/GTTTGG | GATCAG/gtgcctgtt | 8 | 1.4 |
| IX | 179 | attcttgtag/AGCGTT | CTCTGG/gtaagagc | 9 | 0.9 |
| X | 889 | tccctgcag/TCTGAT | AAGCAG/gtcagcacc | 10 | 0.5 |
| XI | 153 | ttcatcgtag/GGCCCT | GAAAAG/gtaaaactg | 11 | 1.6 |
| XII | 194 | tgctggcag/GATCTG | CAGCAG/gtgagcagg | 12 | 4.2 |
| XIII | 88 | ctgttcacag/GTTGAT | GCCCAG/gttggggctc | 13 | 0.5 |
| XIV | 2935 | gcccacag/GAAAAG | | | |

rats and humans (94% homology). To obtain the entire open reading frame of mDab2ip, we performed RT-PCR from RNA isolated from the mouse brain using primer sets based on the rat *DAB2IP* cDNA sequence (Chen *et al*., 2002; Wang *et al*., 2002). The deduced 1065 amino acids of *mDab2ip* revealed a high homology sequence with human and rat counterparts (Fig. 3A). Using the program "NCBI conserved domain database" (http://www.ncbi.nih.gov/structure/cdd/wrpsb.cgi), ScanProsite program (http://au.expasy.org/cgi-bin/scanprosite), and Motif Scan Graphic program (http://scansite.mit.edu), there are five conserved protein domains predicted: PH (pleckstrin homology domain 30–79), C2 (protein kinase C conserved region2 [CalB, amino acid 90–189), RasGAP (GTPase-activating protein, amino acid 212–539), proline-rich domain (amino acid 796–805), and a leucine zipper domain (amino acid 911–932) (Fig. 3B). These data indicate that mDab2ip appears to be a new member of the RasGAP family protein.

### *Expression profile of* mDab2ip *mRNA in different mouse tissues and cell lines*

To determine the tissue distribution of *mDab2ip* mRNA, we performed a real-time RT-PCR analyses (Fig. 4A). Results indicated a unique expression pattern in certain organs. For example, *mDab2ip* was most abundant in the brain (72.5-fold), salivary gland (38.7-fold), and testis (21.3-fold); moderate expression in the kidney (15.0-fold) and heart (11.3-fold); low expression in the lung (7.4-fold), seminal vesicle (7.1-fold), ventral prostate (6.5-fold), epididymis (6.1-fold), liver (5.9-fold), and bladder (5.6-fold); quite low expression in the coagulation gland (3.6-fold) and skeleton muscles (2.0-fold) compared with the spleen, which has the lowest expression level (=1.0) among all the organs tested. This pattern of expression is consistent with our previous report (Wang *et al*., 2002) and gene card expression pattern (http://bioinformatics.weizann.ac.il/cards-bin/arddisp?DAB2IP) except the expression level of *Dab2ip* detected from the heart.

In several established mouse cell lines, we also observed a differential expression level of the *mDab2ip* transcript. In general, the highest level of *mDab2ip* mRNA was detected in the NIH 3T3 cell line (≈8.5-fold higher than TRAMP-C3); TRAMP-C1 and -C2 lines (≈3-fold) had moderate expressions, and the TRAMP-C3 line had the lowest expression (Fig. 4B). PC-3, a human prostate cancer cell line, was used as a negative control (Chen *et al*., 2003).

### *Analysis of the 5′-upstream sequence of the* mDab2ip *gene*

To analyze the promoter region of the *mDab2ip* gene, a 1.3-kb fragment from position −730 to +545 (transcription initial site as +1 predicted by 5′RACE) containing a 5′ upstream region of the exon Ia, exon Ia, and partial intron1a region, was amplified by PCR from clone 22N15 using primer set F1/R2 (Table 1). Sequencing analysis indicated that this region is very GC-rich. Using the TFSEARCH program (http://www.cbrc.jp/research/db/TFSEARCH.html); Promoter Scan II program (http://thr.cit.nih.gov/molbio/proscan/), and MacVector 7.0 program, we identified several potential *trans*-factor binding sites (Fig. 5A) including Sp1, AP-1 AP-2, SREBP, and p300, GATA-1/2, PEA2, AML-1a, and MalT_box. Neither the TATA-box nor the CAAT-box was identified. The similar *trans*-factor binding sites were also detected in the *hDAB2IP* gene (Chen *et al*., 2002). It indicates that the *Dab2ip* gene is a typical TATA-less promoter.

To define the potential promoter region in the *mDab2ip* gene, we examined the reporter gene activities of a series of deletion constructs (Fig. 5B) generated from the clone 22N15. Consistent with Figure 4B, the luciferase activity of the *mDab2ip* promoter constructs was much higher in NIH-3T3 cell than two other mouse prostatic epithelial cells (Fig. 5C).

In both TRAMP-C1 and TRAMP-C3 cells (Fig. 5D), we observed two constructs (i.e., pGL3–F6/R2 [from −421 to +545] and pGL3–F7/R2 [from −147 to +545]) expressed higher luciferase reporter gene activity than that of pGL3–F1/R2 (from −730 to +545), suggesting the presence of a negative *cis*-element between −730 and −421. Moreover, the reporter gene activity decreased significantly in the rest of the deletion constructs (i.e., pGL3–F8/R2, pGL3–F10/R2, and pGL3– F12/R2). Also, very little reporter gene activity was observed in cells transfected with either pGL3–F6/*Nco*I (from −421 to −157) or

A

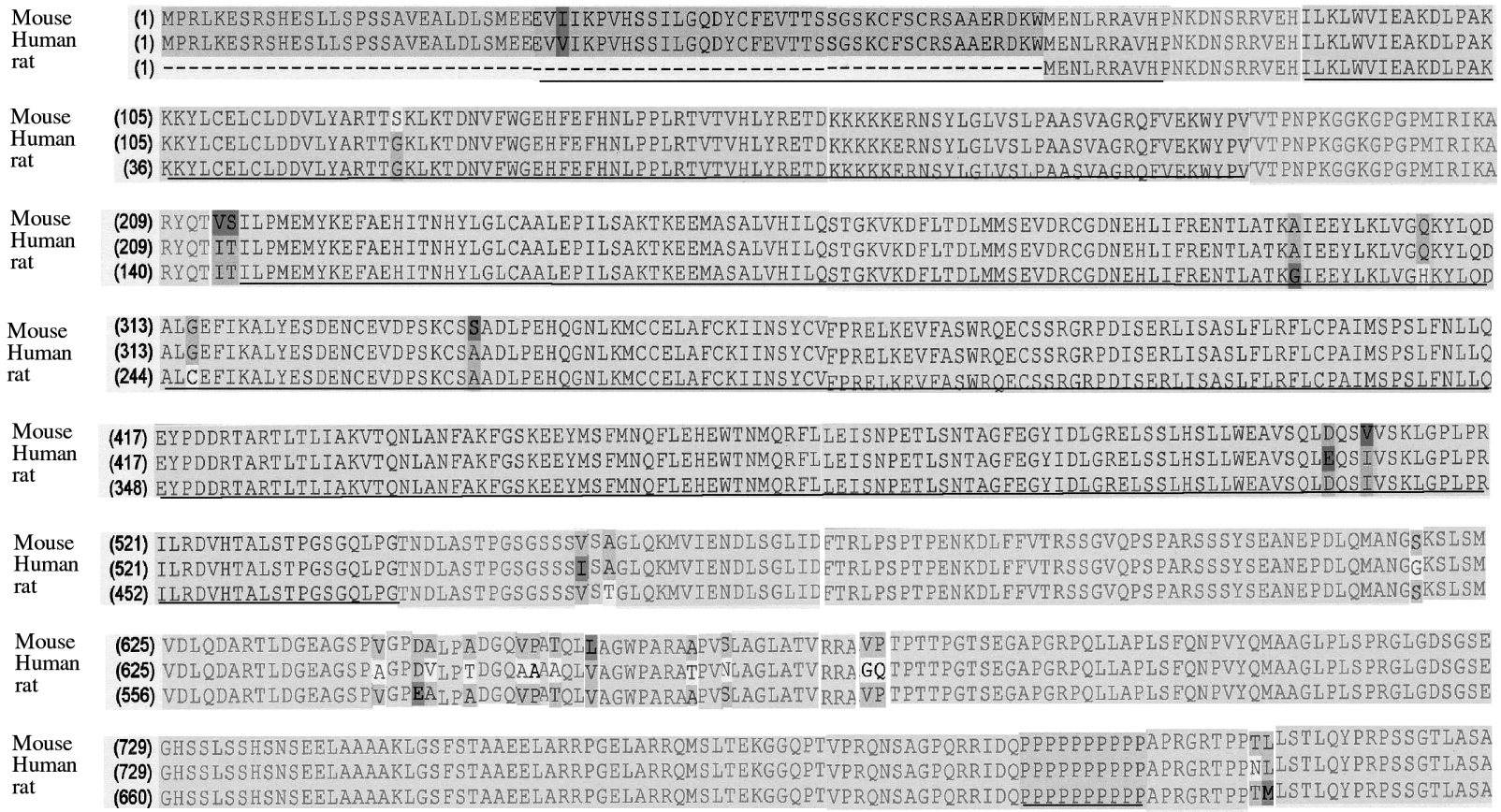
Mouse
Human
rat
(1) MPRLKESRSHESLLSPSSAVEALDLSMEEEVIIKPVHSSILGQDYCFEVTTSSGSKCFSCRSAAERDKWMENLRRAVHPNKDNSRRVEHILKLWVIEAKDLPAK
(1) MPRLKESRSHESLLSPSSAVEALDLSMEEEVVIKPVHSSILGQDYCFEVTTSSGSKCFSCRSAAERDKWMENLRRAVHPNKDNSRRVEHILKLWVIEAKDLPAK
(1) ----------MENLRRAVHPNKDNSRRVEHILKLWVIEAKDLPAK
(105) KKYLCELCLDDVLYARTTSKLKTDNVFWGEHFEFHNLPPLRTVTVHLYRETDKKKKKERNSYLGLVSLPAASVAGRQFVEKWYPVVTPNPKGGKGPGPMIRIKA
(105) KKYLCELCLDDVLYARTTGKLKTDNVFWGEHFEFHNLPPLRTVTVHLYRETDKKKKKERNSYLGLVSLPAASVAGRQFVEKWYPVVTPNPKGGKGPGPMIRIKA
(36) KKYLCELCLDDVLYARTTGKLKTDNVFWGEHFEFHNLPPLRTVTVHLYRETDKKKKKERNSYLGLVSLPAASVAGRQFVEKWYPVVTPNPKGGKGPGPMIRIKA
(209) RYQTVSILPMEMYKEFAEHITNHYLGLCAALEPILSAKTKEEMASALVHILQSTGKVKDFLTDLMMSEVDRCGDNEHLIFRENTLATKAIEEYLKLVGQKYLQD
(209) RYQTITILPMEMYKEFAEHITNHYLGLCAALEPILSAKTKEEMASALVHILQSTGKVKDFLTDLMMSEVDRCGDNEHLIFRENTLATKAIEEYLKLVGQKYLQD
(140) RYQTITILPMEMYKEFAEHITNHYLGLCAALEPILSAKTKEEMASALVHILQSTGKVKDFLTDLMMSEVDRCGDNEHLIFRENTLATKGIEEYLKLVGHKYLQD
(313) ALGEFIKALYESDENCEVDPSKCSSADLPEHQGNLKMCCELAFCKIINSYCVFPRELKEVFASWRQECSSRGRPDISERLISASLFLRFLCPAIMSPSLFNLLQ
(313) ALGEFIKALYESDENCEVDPSKCSAADLPEHQGNLKMCCELAFCKIINSYCVFPRELKEVFASWRQECSSRGRPDISERLISASLFLRFLCPAIMSPSLFNLLQ
(244) ALCEFIKALYESDENCEVDPSKCSAADLPEHQGNLKMCCELAFCKIINSYCVFPRELKEVFASWRQECSSRGRPDISERLISASLFLRFLCPAIMSPSLFNLLQ
(417) EYPDDRTARTLTLIAKVTQNLANFAKFGSKEEYMSFMNQFLEHEWTNMQRFLLEISNPETLSNTAGFEGYIDLGRELSSLHSLLWEAVSQLDQSVVSKLGPLPR
(417) EYPDDRTARTLTLIAKVTQNLANFAKFGSKEEYMSFMNQFLEHEWTNMQRFLLEISNPETLSNTAGFEGYIDLGRELSSLHSLLWEAVSQLEQSIVSKLGPLPR
(348) EYPDDRTARTLTLIAKVTQNLANFAKFGSKEEYMSFMNQFLEHEWTNMQRFLLEISNPETLSNTAGFEGYIDLGRELSSLHSLLWEAVSQLDQSIVSKLGPLPR
(521) ILRDVHTALSTPGSGQLPGTNDLASTPGSGSSSVSAGLQKMVIENDLSGLIDFTRLPSPTPENKDLFFVTRSSGVQPSPARSSSYSEANEPDLQMANGSKSLSM
(521) ILRDVHTALSTPGSGQLPGTNDLASTPGSGSSSISAGLQKMVIENDLSGLIDFTRLPSPTPENKDLFFVTRSSGVQPSPARSSSYSEANEPDLQMANGGKSLSM
(452) ILRDVHTALSTPGSGQLPGTNDLASTPGSGSSSVSTGLQKMVIENDLSGLIDFTRLPSPTPENKDLFFVTRSSGVQPSPARSSSYSEANEPDLQMANGSKSLSM
(625) VDLQDARTLDGEAGSPVGPDALPADGQVPATQLLAGWPARAAPVSLAGLATVRRAVPTPTTPGTSEGAPGRPQLLAPLSFQNPVYQMAAGLPLSPRGLGDSGSE
(625) VDLQDARTLDGEAGSPAGPDVLPTDGQAAAAQLVAGWPARATPVNLAGLATVRRAGQTPTTPGTSEGAPGRPQLLAPLSFQNPVYQMAAGLPLSPRGLGDSGSE
(556) VDLQDARTLDGEAGSPVGPEALPADGQVPATQLVAGWPARAAPVSLAGLATVRRAVPTPTTPGTSEGAPGRPQLLAPLSFQNPVYQMAAGLPLSPRGLGDSGSE
(729) GHSSLSSHSNSEELAAAAKLGSFSTAAEELARRPGELARRQMSLTEKGGQPTVPRQNSAGPQRRIDQPPPPPPPPPPAPRGRTPPTLLSTLQYPRPSSGTLASA
(729) GHSSLSSHSNSEELAAAAKLGSFSTAAEELARRPGELARRQMSLTEKGGQPTVPRQNSAGPQRRIDQPPPPPPPPPPAPRGRTPPNLLSTLQYPRPSSGTLASA
(660) GHSSLSSHSNSEELAAAAKLGSFSTAAEELARRPGELARRQMSLTEKGGQPTVPRQNSAGPQRRIDQPPPPPPPPPPAPRGRTPPTMLSTLQYPRPSSGTLASA

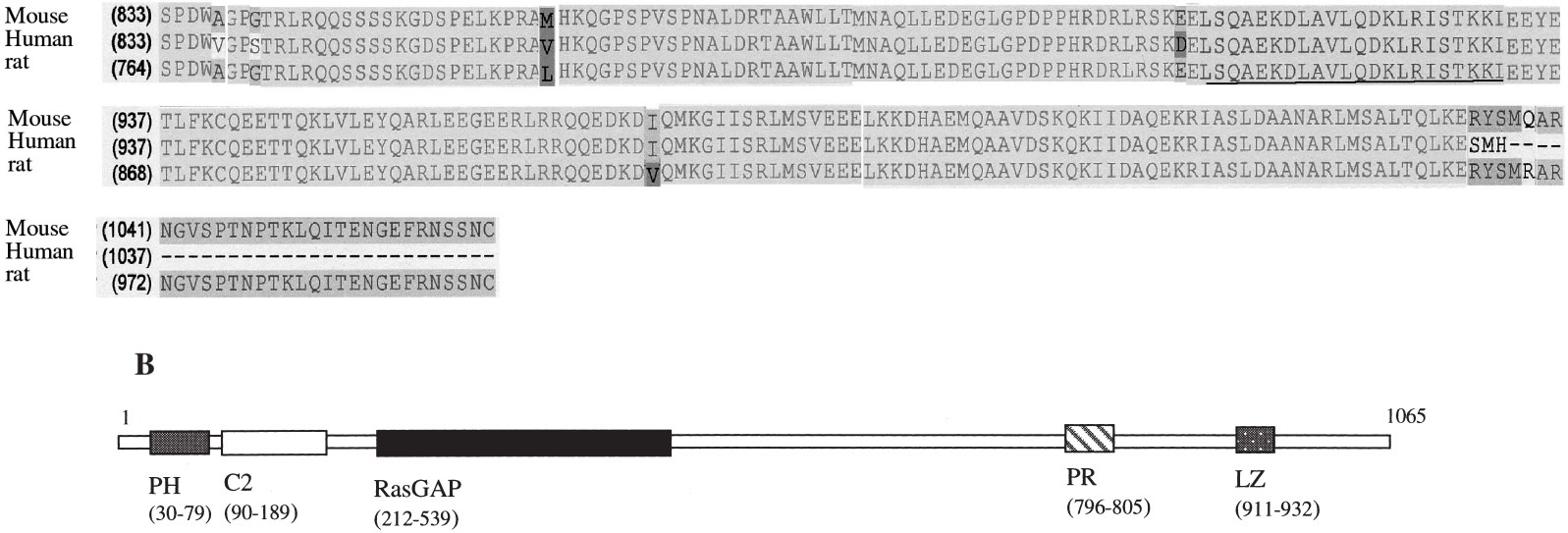


**FIG. 3.** The predicted functional domain of the *mDab2ip* protein. (**A**) Alignment of mouse (m) Dab2IP, human (h), and rat (r) DAB2IP proteins exhibited a high sequence homology. Potential functional domains are shaded and underlined. Shaded letters indicate the nonidentical amino acids. (**B**) Schematic representation of *mDab2ip* protein. PH (peckstrin homology domain, amino acids 30–79); C2 (protein kinase C conserved region 2 domain, amino acids 90–189); RasGAP (Ras GTPase-activator domain, amino acids 212–539); PR (proline-rich domain, amino acids 796–805); and LZ (leucine zipper domain, amino acids 911–932).

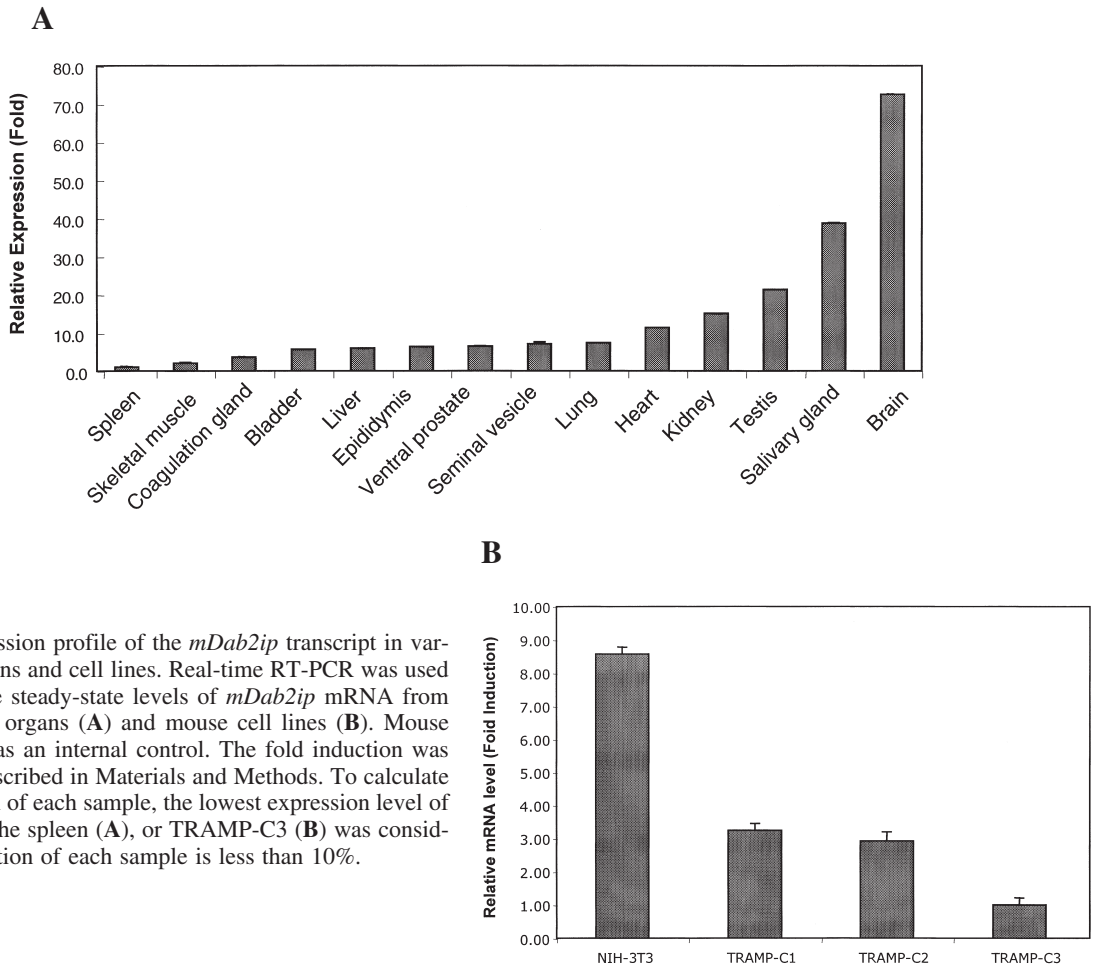


**FIG. 4.** Expression profile of the *mDab2ip* transcript in various mouse organs and cell lines. Real-time RT-PCR was used to determine the steady-state levels of *mDab2ip* mRNA from different mouse organs (**A**) and mouse cell lines (**B**). Mouse actin was used as an internal control. The fold induction was calculated as described in Materials and Methods. To calculate the relative level of each sample, the lowest expression level of *mDab2ip* from the spleen (**A**), or TRAMP-C3 (**B**) was considered as 1. Variation of each sample is less than 10%.

pGL3–F6/*San*DI (from −421 to −97). We therefore conclude that the basal promoter region of the *mDab2ip* gene is between −147 and +545. Noticeably, a good correlation between the *mDab2ip* mRNA level and the reporter gene activity was observed in these TRAMP-C cells, indicating that this is a promoter operative in mouse prostatic epithelial cells.

To further identify the role of *cis*-elements such as Sp1 and AP2 in modulating the basal activity of the *mDab2ip* gene promoter in both TRAMP-C1 and TRAMP-C3 cells, we examined the reporter gene activity from either pGL3–ΔSp1, or pGL3–ΔAP2 in these cells. The luciferase activity of both mutants did not change compared with that of pGL3–F7/R2 in these two cell lines (Fig. 5D), suggesting that either factor is not critical for maintaining the basal *mDab2ip* gene promoter activity in TRAMP-C cells. In contrast, the luciferase activities of both mutants in NIH-3T3 cell line reduced dramatically (Fig. 5E), indicating that that either the Sp1 or AP2 site is critical for *mDab2ip* gene promoter activity in NIH-3T3.

### *Epigenetic regulation of* mDab2ip *promoter activity in prostatic epithelium*

To understand the underlying mechanism(s) leading to the downregulation of *mDab2ip* gene expression in TRAMP-C3 cells, two common epigenetic regulatory pathways (ie., histone acetylation and DNA methylation) were analyzed using epigenetic modifiers such as TSA and 5′-Aza. As shown in Figure 6A, TSA or 5′-Aza could increase *mDab2ip* mRNA levels in the TRAMP-C3 cell in a dose-dependent manner, and the combination exhibited an additive effect, suggesting that both agents might mediate through a similar pathway.

We further investigated whether the status of acetyl histone H3 (H3) in the *mDab2ip* promoter region correlated with the induction of both agents. As shown in Figure 6B, the elevated levels of acetyl H3 associated with the promoter region (from −154 to +7) were detected in TRAMP-C3 cells treated with a single agent or a combination, and the combination of TSA and 5′-Aza could elicit higher acetyl H3 levels than a single agent alone.

Moreover, we examined the DNA methylation status of CpG islands (from +8 to +294 region) of the *mDab2ip* promoter from several mouse prostatic epithelial cells using bisulfite DNA sequencing assay. Data from Figure 6C indicated that DNA methylation was rarely detected at the CpG sites (Fig. 6C). Taken together, we believe that histone acetylation play a more critical role than DNA methylation in modulating the *mDab2ip* gene expression.

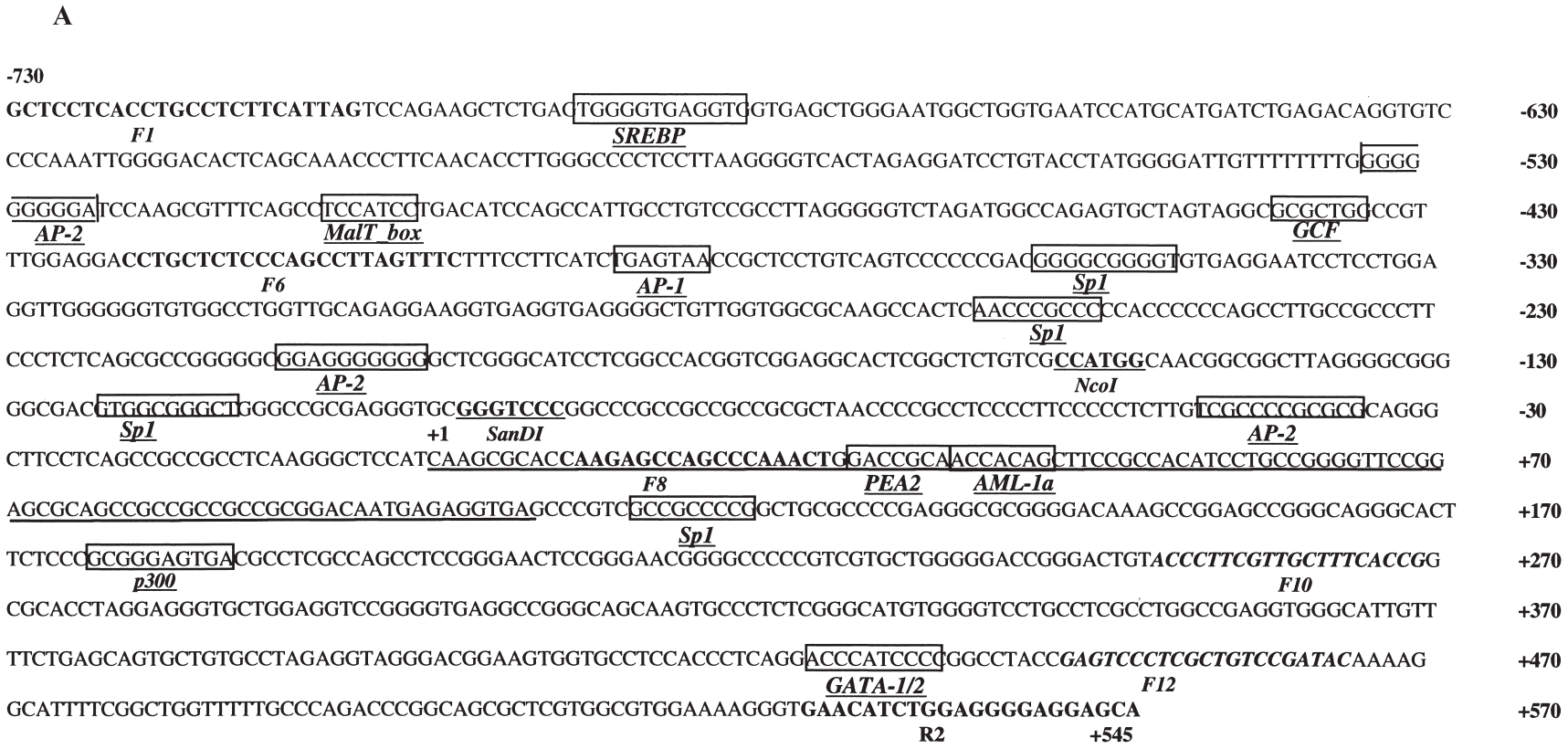


**FIG. 5.** Characterization of the *mDab2ip* gene promoters. (**A**) The predicted regulatory sequences of the *mDab2ip* gene. Exon Ia sequence of the *mDab2ip* is underlined. The putative *cis*-acting elements are boxed. Primer sequences (bold letters) and restriction endonucleases sites (bold letters and underlined) were used in subsequent cloning for reporter constructs. The transcription start site (TSS) as +1 was predicted by 5′ RACE.

(*continued*)

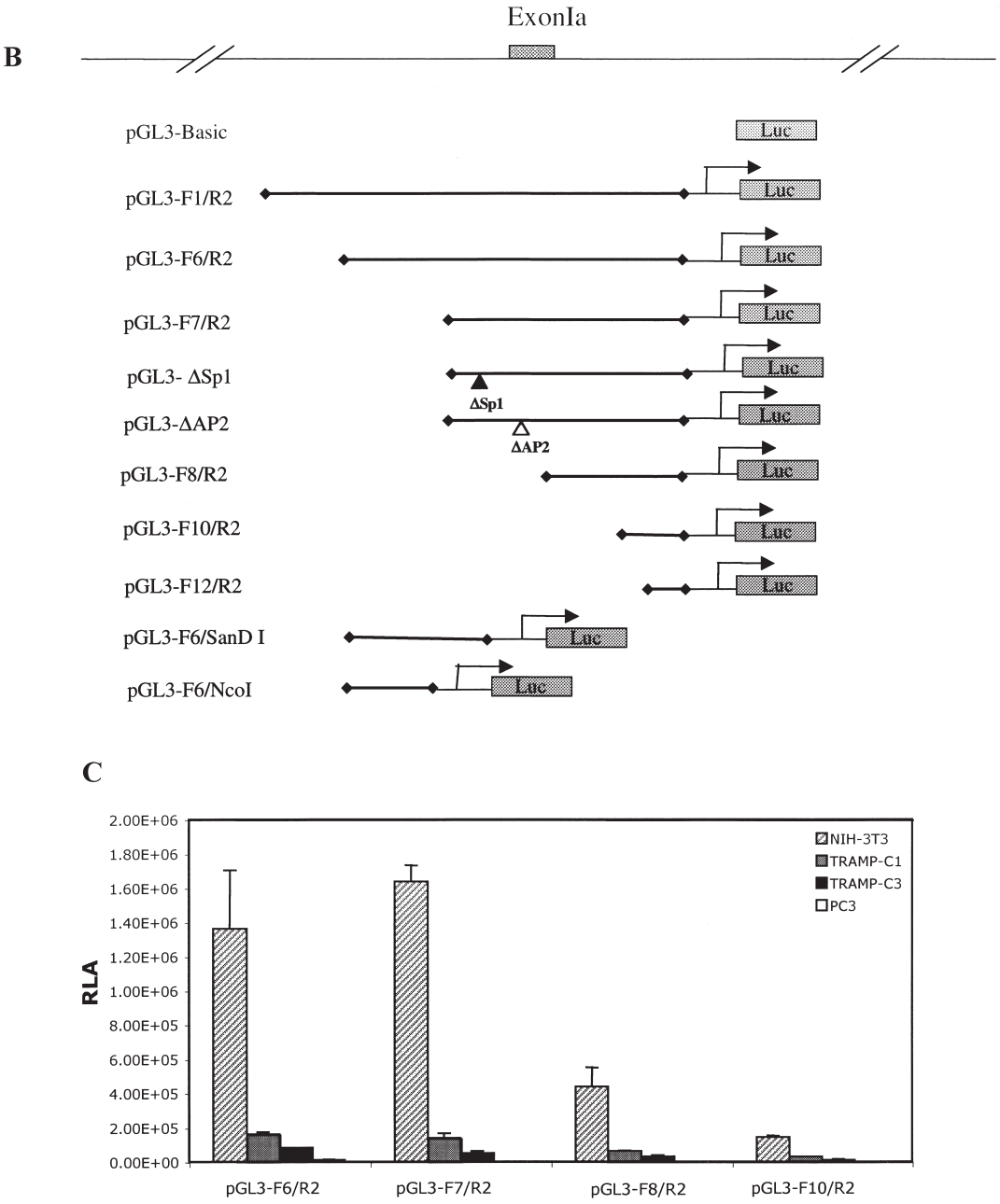


**FIG. 5.** *Continued.* (**B**) Schematic representation of the *mDab2ip* promoter construct. A series of reporter gene constructs were generated by series deletion or removing the potential *cis*-element of the *mDab2ip* promoter sequence using pGL3 as a backbone vector described in Materials and Methods. (**C**) Characterization of *mDab2ip* promoter activity in various mouse cell lines.

## DISCUSSION

The *mDab2ip* gene spans approximately 65 kb, containing 14 exons and 13 introns with at least three variants: exon Ia, exon Ib, and exon Ic found from different sources of RNA using the 5′RACE assay. All three splicing sequences of *mDab2ip* P cDNA have been submitted to the GenBank™ (AY305656 [*mDab2ip* a]; AY 305657 [*mDab2ip* b]; AY305658 [*mDab2ip* c]). Using FISH analysis, *mDab2ip* was localized at chromosome band 2B (Fig. 2), which is consistent with the LocusLink program analysis (http://www.ncbi.nih.gov/ LocusLink).

In this study, we performed a real-time RT-PCR to demonstrate the *mDab2ip* mRNA levels in different organs (Fig. 4A). Very abundant *mDab2ip* mRNA levels were found in the brain, salivary gland, and testis, and the moderate levels were found in the kidney and heart. In addition, organs such as the lung, seminal vesicle, ventral prostate, epididymis, liver, and bladder only express low levels of *Dab2ip* mRNA. Also, the lowest level of *Dab2ip* mRNA was detected in the coagulation gland, skeletal muscles, and spleen. Such a diverse expression pattern of the *Dab2ip* gene implies that *mDab2ip* may have a unique physiological function in a specific organ. To gain the insight of the mechanisms of *mDab2ip* transcriptional regulation, we isolated an ~1.3 kb (Fig. 5A) fragment containing a 5′-upstream region

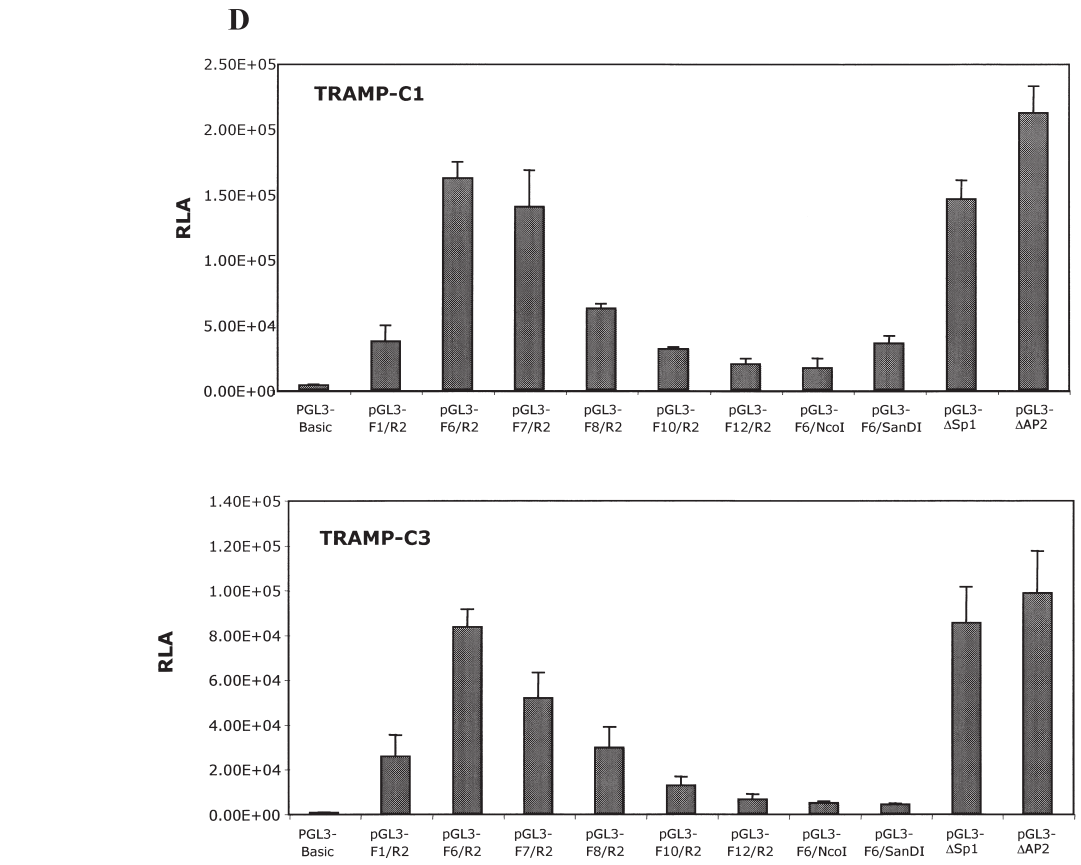


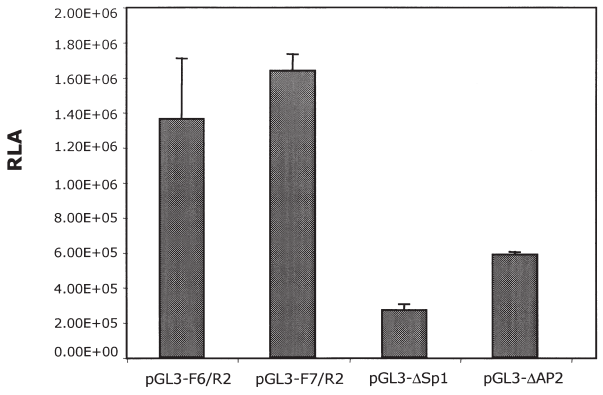


**FIG. 5.** *Continued.* (**D**) Mapping core of the *mDab2ip* promoter region in TRAMP-C1 and TRAMP-C3. (**E**) Evaluating the role of two *cis*-elements (Sp1 and AP2) in modulating *mDab2ip* promoter activity in NIH-3T3 cells. Bars, SD.

from exon Ia, and we found very rich GC-rich sequences and no canonical TATA boxes in this region. Nevertheless, we have shown that the 5′-flanking region from positions −730/+545 could enhance the reporter gene activity, and it contained the basal promoter (−147/+545) and a negative regulatory element (−730/−421) (Fig. 5). In this region, several putative *cis*-elements could underlie the differential *Dab2ip* gene expressions in various organs or cells, so we have employed a series of mutants (Fig. 5D and E) to examine the role of two common *cis*-elements such as Sp1 and AP2 in maintaining the basal promoter activity of the *mDab2ip* gene. In NIH-3T3, both *cis*-elements are critical for maintaining the basal promoter activity of the *mDab2ip* gene (Fig. 5E). However, in prostatic epithelium, either *cis*-element may not play a critical role in modulating the basal promoter activity of the *mDab2ip* gene (Fig. 5D). Instead, the status of histone aceylation but not DNA methylation associated with the *mDab2ip* promoter region correlates with its gene induction in the TRAMP-C3 (Fig. 6). It also appears that 5′-Aza is able to increase the acetylated histone levels associated with the *mDab2ip* promoter region. A similar observation was demonstrated in our previous studies (Chen *et al*., 2003), since it is known that the hypomethylation agent can cause the dissociation of the transcription repressor complex containing both DNMT and HDAC (Jones and Baylin, 2002).

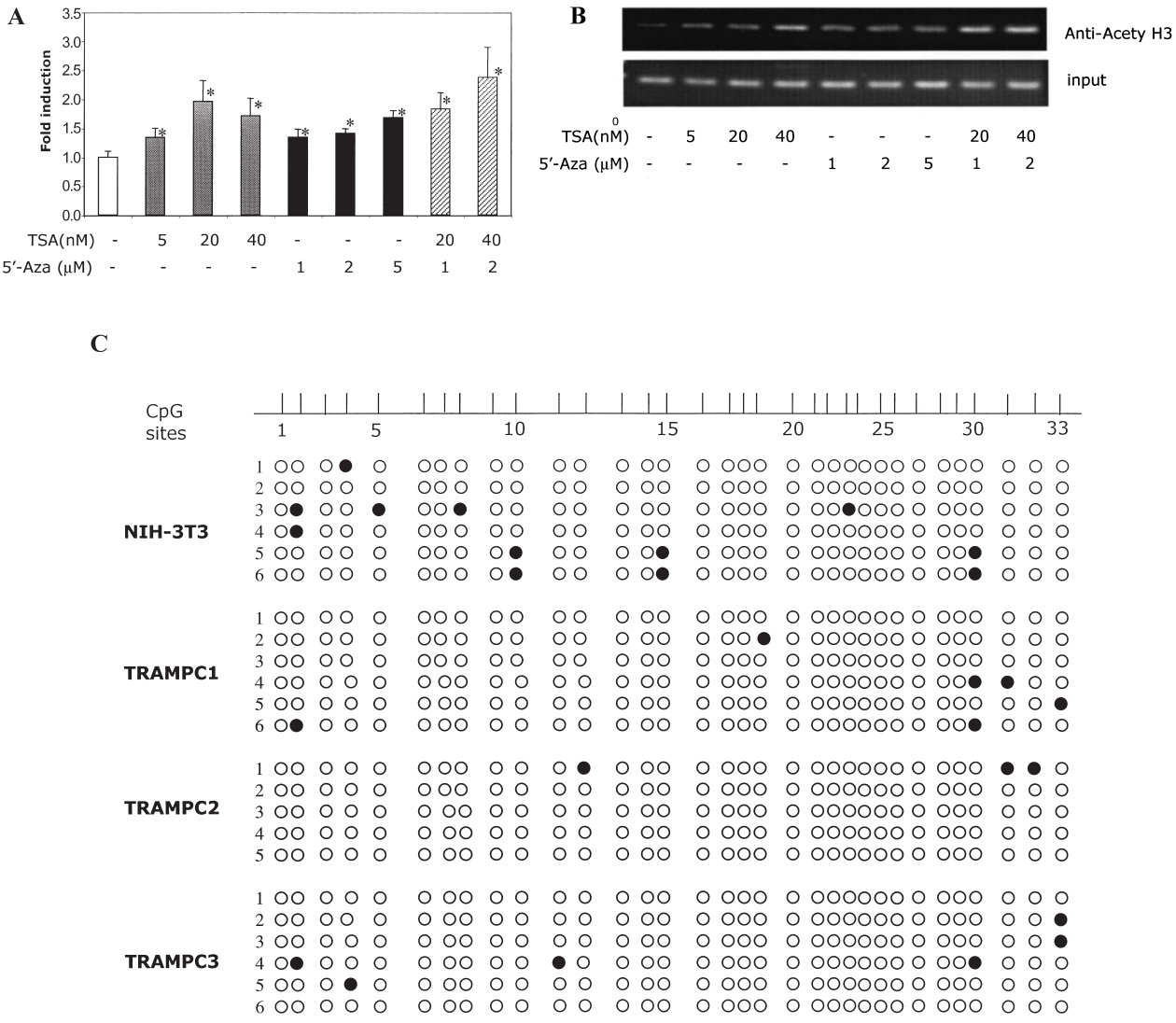


**FIG. 6.** Epigenetic regulation of the *mDab2ip* gene promoter in mouse prostatic epithlium. (**A**) The effect of TSA and/or 5′-Aza on *mDab2ip* mRNA expression in TRAMP-C3 cells. *Statistically significant ($p<$). (**B**) The effect of TSA and/or 5′-Aza on acetyl histone H3 levels associated with the *mDab2ip* promoter in TRAMP-C3 cells. (**C**) Profiling DNA methylation status on the CpG site in the *mDab2ip* gene promoter region (from +8 to +294) in several mouse cell lines. The position of the CpG dinucleotide site (vertical tick) was indicated. ○, unmethylated CpG; ●, methylated CpG.

In our previous publications (Chen *et al*., 2002; Wang *et al*., 2002), we found the translation initiation site (ATG) of *DAB2IP* at 63-bp from the 5′-end of exon 3 and predicted a putative open reading frame encoding the 967-amino acid for hDAB2IP or the 996- amino acid for rat DAB2IP (rDAB2IP). However, the updated sequence data from NCBI (accession no. NP_619723) indicate that an additional ATG site is mapped at 11-bp from the 5′-end of exon 2 that was also detected in *mDab2ip*. Thus, predicted mDab2ip protein encodes the 1065-amino acid containing an additional 69-amino acid with a PH domain. The PH domain is a short motif that mediates membrane localization, and is found in many proteins involved in signal transduction, including GAPs for Ras (Shaw, 1996; Rebecchi and Scarlata, 1998). The predicted protein sequence alignment between mouse and human DAB2IP is remarkably conserved. Von Bergh *et al*. (2004) reported that the *hDAB2IP* is the alias for the *AF9Q34*gene (accession no. AY032952) as a novel fusion partner of MLL in the AML patient with (9:11) translocation. The juxaposition of MLL intron 9 into exon 2 of AF9Q34 will result in the loss of the exon 2 splicing donor site. Consequently, the *hDAB2IP*/AF9Q34 exon 2 sequences will be spliced out and result in an MLL-exon 9/AF9Q34-exon 3 fusion product. In this case, the AF9Q34-MLL fusion protein does not contain the PH domain, implying that the normal function of the AF9Q34 gene may be altered due to the chromosomal translocation.

Sequence analysis of mDab2ip revealed the presence of a highly conserved GAP-related domains (GRD), the catalytic unit to stimulate the GTPase activity of Ras proteins, in the N-terminus of mDab2ip. GRD is a characteristic domain in the all RasGAPs such as human neurofiibromin (NF1), rat SynGAP, p120GAP, and human nGAP (Bernards *et al*., 1992; Davis *et al*., 1993; Li *et al*., 1996; Kim *et al*., 1998; Noto *et al*., 1998;

Glanzer *et al*., 2002). Homayouni *et al*. (2003) suggest that Dab2IP may function as a downstream effector in the Reelin-signaling pathway that influences Ras signaling during brain development. With the cloning of this gene from the mouse, studying the function al role of this gene in brain development as well as prostate carcinogeneis can be feasible.

## ACKNOWLEDGMENTS

We thank Dr. Norman Greenberg (Baylor College of Medicine) for providing TRAMP-C cell lines, and Kenneth S. Koeneman (UT Southwestern Medical Center) for reading this manuscript. This work is supported in part by United States Army Grants W81XWH-04-1-0222 and DAMD17-03-2-0033. Sequence data from this article have been deposited into the EMBL/GenBank Data Libraries under accession number AY305656, AY305657, and AY305658.

## REFERENCES

BERNARDS, A., HAASE, V.H., MURTHY, A.E., MENON, A., HANNIGAN, G.E., and GUSELLA, J.F. (1992). Complete human NF1 cDNA sequence: two alternatively spliced mRNAs and absence of expression in a meuroblastoma line. DNA Cell Biol. **11,** 727–734.

CHEN, H., PONG, R.C., WANG, Z., and HSIEH, J.T. (2002). Differential regulation of the human gene DAB2IP in normal and malignant prostatic epithelia: Cloning and characterization. Genomics **79,** 573–581.

CHEN, H., TOYOOKA, S., GAZDAR, A. F., and HSIEH, J.T. (2003). Epigenetic regulation of a novel tumor suppressor gene (*hDAB2IP*) in prostate cancer cell lines. J. Biol. Chem. **278,** 3121–3130.

DAVIS, M. M., CATINO, J.J., SATOH, T., KAZIRO, Y., and PERKINS, L.M. (1993). Sequence of the cDNA encoding Ras GTPase-activating protein from rat. Gene **134,** 305–306.

DOTE, H., TOYOOKA, S., TSUKUDA, K., YANO, M., OUCHIDA, M., DOIHARA, H., SUZUKI, M., CHEN, H., HSIEH, J.T., GAZDAR, A.F., *et al*. (2004). Aberrant promoter methylation in human DAB2 interactive protein (*hDAB2IP*) gene in breast cancer. Clin. Cancer Res. **10,** 2082–2089.

FOSTER, B.A., GINGRICH, J.R., KWON, E.D., MADIAS, C., and GREENBERG, N.M. (1997). Characterization of prostatic epithelial cell lines derived from transgenic adenocarcinoma of the mouse prostate (TRAMP) model. Cancer Res. **57,** 3325–3330.

FULOP, V., COLITTI, C.V., GENEST, D., BERKOWITZ, R.S., YIU, G.K., NG, S.W., SZEPESI, J., and MOK, S.C. (1998). DOC-2/hDAB2, a candidate tumor suppressor gene involved in the development of gestational trophoblastic diseases. Oncogene **17,** 419–424.

GLANZER, J.G., LIAO, L., BAKER, T., MCMULLEN, M.H., LANGAN, A.S., CRANDALL, L.Z., and VORCE, R.L. (2002). Organization and regulation of the human rasGAP gene. Gene **285,** 149–156.

GINGRICH, J.R., BARRIOS, R.J., KATTAN, M.W., NAHM, H.S., FINEGOLD, M.J., and GREENBERG, N.M. (1997). Androgen-independent prostate cancer progression in the TRAMP model. Cancer Res. **57,** 4687–4691.

GREENBERG, N.M., DEMAYO, F., FINEGOLD, M.J., MEDINA, D., TILLEY, W.D., ASPINALL, J.O., CUNHA, G.R., DONJACOUR, A.A., MATUSIK, R.J., and ROSEN, J.M. (1995). Prostate cancer in a transgenic mouse. Proc. Natl. Acad. Sci. USA **92,** 3439–3443.

HOMAYOUNI, R., MAGDALENO, S., KESHVARA, L., RICE, D. S., and CURRAN, T. (2003). Interaction of Disabled-1 and the GTPase activating protein Dab2IP in mouse brain. Mol. Brain Res. **115,** 121–129.

JONES P.A., and BAYLIN, S.B. (2002). The fundamental role of epigenetic events in cancer. Nat. Rev. **3,** 415–428.

JONES, P.A., and TAKAI, D. (2001). The role of DNA methylation in mammalian epigenetics. Science **293,** 1068–1070.

KIM, J.H., LIAO, D., LAU, L.F., and HUGANIR, R. (1998). SynGAP: A synaptic RasGAP that associates with the PSD-95/SAP90 protein family. Neuron **20,** 683–691.

LI, S., SATOH, H., WATANABE, T., NAKAMURA, S., and HATTORI, S. (1996). cDNA cloning and chromosomal mapping of a novel human GAP (GAP1M), a GTPase-activating protein of Ras. Genomics **35,** 625–627.

NOTO, S., MAEDA, T., HATTORI, S., INAZAWA, J., IMAMURA, M., ASAKA, M., and HATAKEYAMA, M. (1998). A novel human RasGAP-like gene that maps within the prostate cancer susceptibility locus at chromosome 1q25. FEBS Lett. **441**, 127–131.

REBECCHI, M.J., and SCARLATA, S. (1998). Pleckstrin homology domains: A common fold with diverse functions. Annu. Rev. Biophys. Biomol. Struct. **27,** 503–528.

SHAW, G. (1996). The pleckstrin homology domain: An intriguing multifunctional protein module. Bioessays **18,** 35–46.

TSENG, C.P., ELY, B.D., PONG, R.C., WANG, Z., ZHOU, J., and HSIEH, J.T. (1999). The role of DOC-2/DAB2 protein phosphorylation in the inhibition of AP-1 activity. An underlying mechanism of its tumor-suppressive function in prostate cancer. J. Biol. Chem. **274,** 31981–31986.

VON BERGH, A.R., WIJERS, P.M., GROOT, A.J., VAN ZELDEREN-BHOLA, S., FALKENBURG, J.H., KLUIN, P.M., and SCHUURING, E. (2004). Identification of a novel RAS GTPase-activating protein (*RASGAP*) gene at 9q34 as an *MLL* fusion partner in a patient with de novo acute myeloid leukemia. Genes Chromosomes Cancer **39,** 324–334.

WANG, Z., TSENG, C.P., PONG, R.C., CHEN, H., MCCONNELL, J.D., NAVONE, N., and HSIEH, J.T. (2002). The mechanism of growth-inhibitory effect of DOC-2/DAB2 in prostate cancer. Characterization of a novel GTPase-activating protein associated with N-terminal domain of DOC-2/DAB2. J. Biol. Chem. **277,** 12622–12631.

WOLFFE, A.P., and MATZKE, M.A. (1999). Epigenetics: Regulation through repression. Science **286,** 481–486.

ZHANG, H., ZHANG, R., LUO, Y., D'ALESSIO, A., POBER, J. S., and MIN, W. (2004). AIP1/DAB2IP, a novel member of the Ras-GAP family, transduces TRAF2-induced ASK1-JNK Activation. J. Biol. Chem. **279,** 44955–44965.

ZHANG, R., HE, X., LIU, W., LU, M., HSIEH, J.T., and MIN, W. (2003). AIP1 mediates TNF-$\alpha$-induced ASK1 activation by facilitating dissociation of ASK1 from its inhibitor 14-3-3. J. Clin. Invest. **111,** 1933–1943.

ZHOU, J., and HSIEH J.T. (2001). The inhibitory role of DOC-2/DAB2 in growth factor receptor-mediated signal cascade. DOC-2/DAB2-mediated inhibition of ERK phosphorylation via binding to Grb2. J. Biol. Chem. **276,** 27793–27798.

ZHOU, J., SCHOLES, J., and HSIEH, J.T. (2003). Characterization of a novel negative regulator (DOC-2/DAB2) of c-Src in normal prostatic epithelium and cancer. J. Biol. Chem. **278,** 6936–6941.

Address reprint requests to:
*J.-T. Hsieh, Ph.D.*
*Department of Urology*
*University of Texas Southwestern Medical Center*
*5323 Harry Hines Blvd.*
*Dallas, TX 75390-9110*

*E-mail:* JT.Hsieh@UTSouthwestern.edu

Received for publication June 12, 2005; received in revised form August 15, 2005; accepted January 17, 2006.